

Synthesis of Organic Chromophores for Dye Sensitized Solar Cells

Daniel Hagberg



**KTH Chemical Science
and Engineering**

Licentiate Thesis

Stockholm 2008

Akademisk avhandling som med tillstånd av Kungl Tekniska Högskolan i Stockholm framlägges till offentlig granskning för avläggande av licentiatexamen i kemi med inriktning mot organisk kemi fredagen den 25 januari kl 13.00 i sal D3, KTH, Lindstedtsvägen 5, Stockholm. Avhandlingen försvaras på engelska.

ISBN 978-91-7178-833-7
ISSN 1654-1081
TRITA-CHE-Report 2007:86

© Daniel Hagberg, 2007
Universitetservice US AB, Stockholm

Daniel Hagberg, 2007: "Synthesis of Organic Chromophores for Dye Sensitized Solar Cells" Organic Chemistry, KTH Chemical Science and Engineering, Royal Institute of Technology, SE-100 44 Stockholm, Sweden.

Abstract

This thesis is divided into four parts with organic chromophores for dye sensitized solar cells as the common feature and an introduction with general concepts of the dye sensitized solar cells.

The first part of the thesis describes the development of an efficient organic chromophore for dye sensitized solar cells. The chromophore consists of a triphenylamine moiety as an electron donor, a conjugated linker with a thiophene moiety and cyanoacrylic acid as an electron acceptor and anchoring group. During this work a strategy to obtain an efficient sensitizer was developed. Alternating the donor, linker or acceptor moieties independently, would give us the tool to tune the HOMO and LUMO energy levels of the chromophores. The following parts of this thesis regard this development strategy.

The second part describes the contributions to the HOMO and LUMO energy levels when alternating the linker moiety. By varying the linker the HOMO and LUMO energy levels was indeed shifted. Unexpected effects of the solar cell performances when increasing the linker length were revealed, however.

The third part describes the investigation of an alternative acceptor group, rhodanine-3-acetic acid, in combination with different linker lengths. The HOMO and LUMO energy level tuning was once again successfully shifted. The poor electronic coupling of the acceptor group to the semiconductor surface proved to be a problem for the overall efficiency of the solar cell, however.

The fourth part describes the contributions from different donor groups to the HOMO and LUMO energy levels and has so far been the most successful in terms of reaching high efficiencies in the solar cell. A top overall efficiency of 7.1 % was achieved.

Keywords: Acceptor, chromophore, donor, dye sensitized solar cell, HOMO and LUMO energy level tuning, linker, organic dye.

Abbreviations

DSC	dye sensitized solar cell
CD	cyclodextrin
CE	counter electrode
CV	cyclic voltammetry
dppf	diphenylphosphinoferrocene
FMO	frontier molecular orbital
IPCE	incident photon to current efficiency
LHE	light harvesting efficiency
PIA	photoinduced absorption spectroscopy
spiro-OMeTAD	2,2',7,7'-tetrakis(N, N-di-p-methoxyphenyl-amine)-9,9'-spirobifluorene
SWV	square wave voltammetry
TBAOH	tetrabutylammonium hydroxide
TPA	triphenylamine
<i>quant.</i>	quantitative yield
V_{oc}	open circuit voltage
WE	working electrode

List of Publications

This thesis is based on the following papers, referred to in the text by their Roman numerals **I-V**:

I. A novel organic chromophore for dye-sensitized nanostructured solar cells

Daniel P. Hagberg, Tomas Edvinsson, Tannia Marinado, Gerrit Boschloo, Anders Hagfeldt and Licheng Sun
Chem. Commun. **2006**, 2245-2247

II. Tuning the HOMO and LUMO Energy Levels of Organic Chromophores For Dye Sensitized Solar Cells

Daniel P. Hagberg, Tannia Marinado, Karl Martin Karlsson, Kazuteru Nonomura, Peng Qin, Gerrit Boschloo, Tore Brinck, Anders Hagfeldt and Licheng Sun
J. Org. Chem. **2007**, 72, 9550-9556.

III. Energy level tuning of organic dyes for fundamental studies of the oxide/dye/electrolyte interface in solar cells

Tannia Marinado, Daniel P Hagberg, Tomas Edvinsson, Tore Brinck, Gerrit Boschloo, Haining Tian, Xichuan Yang, Licheng Sun and Anders Hagfeldt
Manuscript

IV. Molecular engineering of Organic Chromophores for dye sensitized cell applications

Daniel P. Hagberg, Jun-Ho Yum, Hyojoong Lee, Filippo De Angelis, Tannia Marinado, Karl Martin Karlsson, Robin Humphry-Baker, Licheng Sun, Andreas Hagfeldt, Michael Grätzel and Md. K. Nazeeruddin
Manuscript

Paper not included in this thesis:

V. Electronic and Molecular Surface Structure of a Polyene-Diphenylaniline Dye Adsorbed from Solution onto Nanoporous TiO₂.

Erik M. J. Johansson, Tomas Edvinsson, Michael Odelius, Daniel P. Hagberg, Licheng Sun, Anders Hagfeldt, Hans Siegbahn and Håkan Renemo, *J. Phys. Chem. C*, **2007**, 111, 8580-8587.

Table of Contents

Abstract

Abbreviations

List of publications

1.	Introduction	1
1.1.	The Dye Sensitized Solar Cell (DSC)	2
1.1.1.	Incident Photon to Current Efficiency (IPCE)	3
1.1.2.	Overall Efficiency of the Photovoltaic Cell (η_{cell})	4
1.2.	Chromophores	4
1.2.1.	Ruthenium Based Chromophores	4
1.2.2.	Organic Chromophores	5
1.2.3.	Solid State Dye Sensitized Solar Cells	8
1.3.	The Aim of This Thesis	8
2.	Donor-Linker-Acceptor Systems: Synthesis of a Triphenylamine Based Dye	9
2.1.	Introduction	9
2.1.1.	Triarylamine in Conducting Materials	9
2.1.2.	Thiophenes as π -Conjugated Linker	10
2.1.3.	Cyanoacrylic Acid as Acceptor and Anchoring Group	11
2.1.4.	Aim of the Study and Synthetic Strategy	12
2.2.	TPA Based Dye (D5) for DSCs	12
2.2.1.	Synthesis of D5	12
2.2.2.	Solar Cell Performance of D5	13
2.3.	Conclusions	16
3.	Linker Variation of TPA Based Chromophores: Synthesis of π -Conjugated Thiophene Dyes	17
3.1.	Introduction	17
3.1.1.	Aim of the Study	17
3.2.	Extended π -Conjugation in TPA Based Dyes	18
3.2.1.	Synthesis of Linker Series	18
3.2.2.	Solar Cell Performance of Linker Series	19
3.3.	Conclusions	22
4.	Acceptor Group Modification and Linker Variation of TPA Based Chromophores: Synthesis of Rhodanine-3-acetic Acid Dyes	25
4.1.	Introduction	25
4.1.1.	Aim of the Study and Synthetic Strategy	25
4.2.	Acceptor Group Modification of Chromophores for DSC Applications	26
4.2.1.	Synthesis of Linker-Acceptor Series	26
4.2.2.	Solar Cell Performance of Linker-Acceptor Series	26
4.3.	Conclusions	29

5.	Donor Variation of TPA Based Chromophores: Synthesis of Different TPA Based Donors	31
5.1.	Introduction	31
5.1.1.	Aim of the Study and Synthetic Strategy	31
5.2.	Donor Modification of Chromophores for DSC Applications	32
5.2.1.	Synthesis of Linker Series	32
5.2.2.	Solar Cell Performance of Donor Series	34
5.2.3.	Solid State Solar Cell Performance of Donor Series	35
5.3.	Conclutions	36
6.	Future Prospects	37
7.	Concluding Remarks	39

Acknowledgements

Appendices

Till Pappa

1. Introduction

*“More energy from sunlight strikes Earth in 1 hour than all of the energy consumed by humans in an entire year.”*¹

The quality of human life is to a large extent dependent on the availability of energy sources. The present annual worldwide energy consumption has already reached a level of over $4 \cdot 10^{18}$ Joules and is predicted to increase rapidly with the increasing world population and the rising demand of energy in the developing countries.² By meeting this energy demand with further depletion of fossil fuel reserves, the environmental damages followed by the enhanced green house effect, caused by the combustion of fossil fuels, could get out of hand. If, on other hand, this energy demand could be met by the use of renewable energy sources the environmental cost could be decreased.

The sun could annually supply the earth with $3 \cdot 10^{24}$ Joules, which is about 750000 times more than the global population currently consumes.³ The dream to capture the sunlight and turn it into electric power or to generate chemical fuels, such as hydrogen, has in the last couple of decades become reality. Colloids and nanocrystalline films of several semiconductor systems have been employed in the direct conversion of solar energy into chemical or electrical energy.⁴ The conventional photovoltaics, based on the solid-state junction devices, such as crystalline or amorphous silicon, has exceptional solar energy conversion to electricity efficiencies of approximately 20%.⁵ However, the fabrication of these photovoltaics is expensive, using energy intensive high temperature and high vacuum processes.

In 1991 O'Regan and Grätzel published a breakthrough of an alternative solar harvesting device, yielding a solar energy conversion to electricity of 7%, based on a mesoscopic inorganic semiconductor.³ Until then, an energy efficiency of 2.5% had been reached in this research field, in which a semiconductor surface such as TiO_2 or ZnO is sensitized with an optical

¹ Lewis, N. S. *Science*, **2007**, *315*, 798-801.

² Grätzel, M. *Chem. Lett.* **2005**, *34*, 8-13.

³ O'Regan, B.; Grätzel, M. *Nature*, **1991**, *353*, 737-740.

⁴ (a) Bard A.J. *J. Phys. Chem.* **1982**, *86*, 172-177. (b) Hagfeldt, A. Grätzel, M. *Chem. Rev.* **1995**, *95*, 49-68.

⁵ Bignozzi, C.A.; Argazzi, R.; Kleverlaan, C.J. *Chem. Soc. Rev.* **2000**, *29*, 87-96.

absorbing chromophore with charge separation properties that can harvest the solar light and in its excited state inject electrons into the semiconductor.⁶

1.1. The Dye Sensitized Solar Cell (DSC)

The DSC, or the Grätzel cell, is a complex system where three different components, the semiconductor, the chromophore and the electrolyte are brought together to generate electric power from light without suffering any permanent chemical transformation (figure 1).⁷

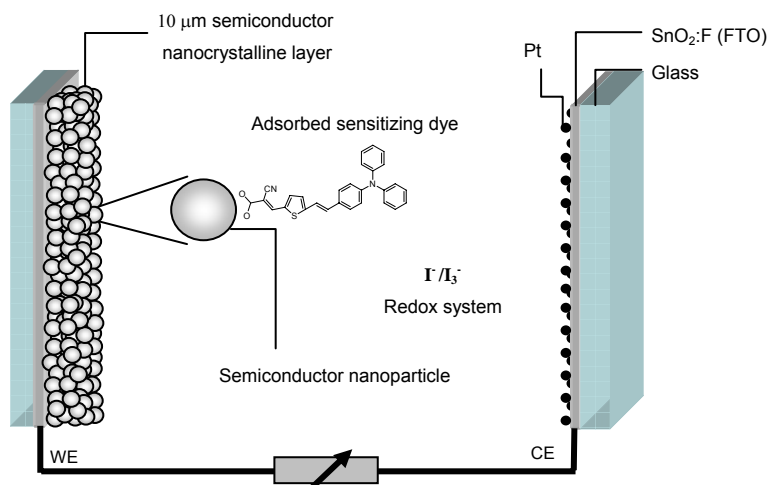


Figure 1. Schematic picture of the Dye Sensitized Solar Cell.

The nanocrystalline semiconductor is usually TiO_2 , although alternative wide bandgap oxides such as ZnO can be used. A monolayer of the chromophore, i.e. the sensitizer, is attached to the surface of the semiconductor. Photoexcitation of the chromophore results in the injection of an electron into the conduction band of the semiconductor (figure 2). The chromophore is regenerated by the electrolyte, usually an organic solvent containing a redox couple, such as iodide/triiodide. The electron donation to the chromophore by iodide is compensated by the reduction of triiodide at the counter electrode and the circuit is completed by electron migration through the external load. The overall voltage generated corresponds to the difference between the Fermi level of the semiconductor and the redox potential of the electrolyte.

⁶ Matsumura, M.; Matsudaira, S.; Tsubomura, H.; Takata, M.; Yanagida, H. *Ind. Eng. Chem. Prod. Res. Dev.* **1980**, *19*, 415-421.

⁷ Grätzel, M.; *Inorg. Chem.* **2005**, *44*, 6841-6851.

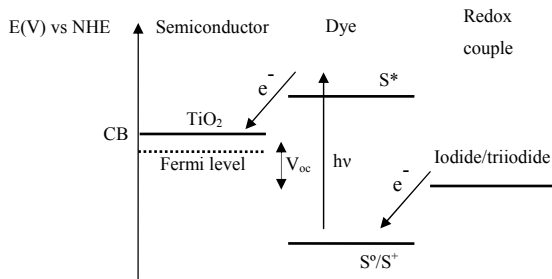


Figure 2. Schematic picture of the electron flow in the DSC.

The performance of the solar cell can be quantified with parameters such as incident photon to current efficiency (IPCE), open circuit photovoltage (V_{oc}) and the overall efficiency of the photovoltaic cell (η_{cell}). The efficiency of the DSC is related to a large number of parameters. This thesis will only focus on the development of efficient sensitizers and their synthesis, even so, it is important to have the general concepts in mind.

1.1.1. Incident Photon to Current Efficiency (IPCE)

IPCE is a parameter to directly measure how efficiently the incident photons are converted to electrons. The wavelength-dependent IPCE can be expressed as the product of the light harvesting efficiency (LHE), quantum yield of charge injection (Φ_{inj}), charge collection efficiency (η_{coll}) at the back contact and quantum yield of regeneration (Φ_{reg}) (eq. 1).

$$IPCE = LHE \cdot \Phi_{inj} \cdot \eta_{coll} \cdot \Phi_{reg} \quad (1)$$

While Φ and η are dependent on kinetic parameters, LHE depends on the active surface area of the semiconductor and on the light absorption of the molecular sensitizers.⁸ In practice the IPCE measurements are performed with monochromatic light and calculated according to eq. 2,

$$IPCE(\%) = \frac{1240 \cdot J_{ph}}{\lambda \cdot \Phi} \cdot 100 \quad (2)$$

where J_{ph} is the short-circuit photocurrent density for monochromatic irradiation and λ and Φ are the wavelength and the intensity, respectively.

⁸ Bignozzi, C. A.; Schoonover J. R.; Scandola, F. *Progr. Inorg. Chem.*, **1997**, *44*, 1-95.

1.1.2. Overall Efficiency of the Photovoltaic Cell (η_{cell})

The solar energy to electricity conversion efficiency is given by eq. 3,

$$\eta_{cell} = \frac{J_{ph} \cdot V_{oc} \cdot ff}{\Phi} \quad (3)$$

where J_{ph} is the short circuit photocurrent density, V_{oc} the open circuit voltage, ff the cell fill factor and Φ the intensity of the incident light.

1.2. Chromophores

The efficiencies of the sensitizers are related to some basic criteria.⁹ The HOMO potential of the dye should be sufficiently positive compared to the electrolyte redox potential for efficient dye regeneration.¹⁰ The LUMO potential of the dye should be sufficiently negative to match the potential of the conduction band edge of the TiO₂ and the light absorption in the visible region should be efficient.⁵ However, by broadening the absorption spectra the difference in the potentials of the HOMO and the LUMO energy levels is decreased. If the HOMO and LUMO energy levels are too close in potential, the driving force for electron injection into the semiconductor or regeneration of the dye from the electrolyte could be hindered. The sensitizer should also exhibit small reorganization energy for excited- and ground-state redox processes, in order to minimize free energy losses in primary and secondary electron transfer steps.

1.2.1. Ruthenium Based Chromophores

Chromophores of ruthenium complexes such as the **N3/N719**^{11,12} dyes and the black dye¹³ have been intensively investigated and show record solar energy-to-electricity conversion efficiencies (η) of 11% (figure 3).

⁹ Kim, S.; Lee, J.K.; Kang, S.O.; Ko, J.; Yum, J.H.; Fantacci, S.; De Angelis, F.; Di Censo, D.; Nazeeruddin, M.K.; Grätzel, M. *J. Am. Chem. Soc.* **2006**, *128*, 16701-16707.

¹⁰ Qin, P.; Yang, X.; Chen, R.; Sun, L.C.; Marinado, T.; Edvinsson, T.; Boschloo, G.; Hagfeldt, A. *J. Phys. Chem. C*, **2007**, *111*, 1853-1860.

¹¹ Nazeeruddin, M. K.; Kay, A.; Rodicio, I.; Humphrybaker, R.; Muller, E.; Liska, P.; Vlachopoulos, N.; Grätzel, M., *J. Am. Chem. Soc.* **1993**, *115*, 6382-6390.

¹² Nazeeruddin, M. K.; Zakeeruddin, S. M.; Humphry-Baker, R.; Jirousek, M.; Liska, P.; Vlachopoulos, N.; Shklover, V.; Fischer, C. H.; Grätzel, M., *Inorg. Chem.* **1999**, *38*, 6298-6305.

¹³ Nazeeruddin, M. K.; Pechy, P.; Renouard, T.; Zakeeruddin, S. M.; Humphry-Baker, R.; Comte, P.; Liska, P.; Cevey, L.; Costa, E.; Shklover, V.; Spiccia, L.; Deacon, G. B.; Bignozzi, C. A.; Grätzel, M., *J. Am. Chem. Soc.* **2001**, *123*, 1613-1624.

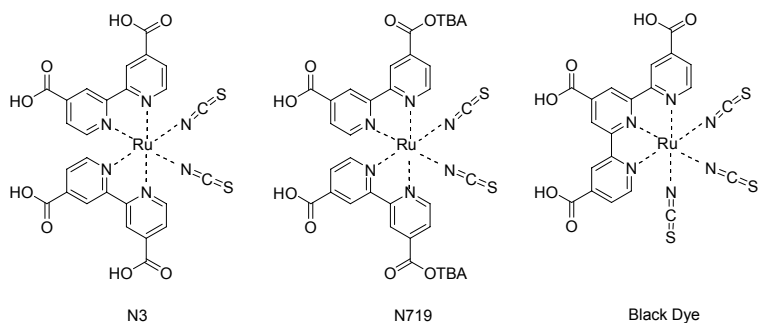


Figure 3. Record performing Ruthenium sensitizers

A large number of different ruthenium based sensitizers have been investigated in order to improve the photovoltaic performance and stability of the DSCs.^{7,14} Amongst them especially two (**K19** and **K77**) have shown interesting properties in that they are competing in efficiency and have higher molar extinction coefficients than the three former (figure 4).¹⁵ The enhanced absorption observed is expected from the extended conjugated system.¹⁶

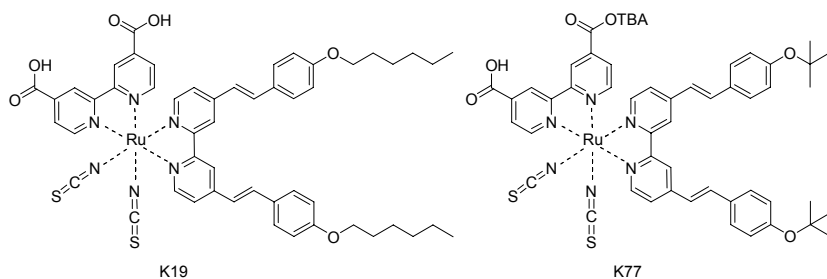


Figure 4. Novel high performing Ruthenium sensitizers

1.2.2. Organic Chromophores

The interest in metal-free organic sensitizers has grown in the past years. In 2000 Sayama et al. published a merocyanine dye (**Mb(18)-N**) which gave an

¹⁴ (a) Chen, C.Y.; Wu, S.J.; Wu, C.G.; Chen, J.G.; Ho, K.C. *Angew. Chem. Int. Ed.* **2006**, *45*, 5822-5825. (b) Jiang, K.J.; Masaki, N.; Xia, J.; Noda, S.; Yanagida, S.; *Chem. Commun.* **2006**, 2460-2462. (c) Hara, K.; Sugihara, H.; Tachibana, Y.; Islam, A.; Yanagida, M.; Sayama, K.; Arakawa, H. *Langmuir* **2001**, *17*, 5992-5999.

¹⁵ (a) Wang, P.; Klein, C.; Humphry-Baker, R.; Zakeeruddin, S. M.; Grätzel, M. *J. Am. Chem. Soc.* **2005**, *127*, 808-809. (b) Kuang, D.; Klein, C.; Ito, S.; Moser, J. E.; Humphry-Baker, R.; Evans, N.; Duriaux, F.; Grätzel, C.; Zakeeruddin, S. M.; Grätzel, M.; *Adv. Mater.* **2007**, *19*, 1133-1137.

¹⁶ Aranyos, V.; Hjelm, J.; Hagfeldt, A.; Grennberg, H. *J. Chem. Soc., Dalton trans.* **2004**, 1319-1325.

efficiency of 4.2% (figure 5).¹⁷ Before this milestone, the organic dyes for DSCs performed relatively low efficiencies ($\eta < 1.3\%$).¹⁸

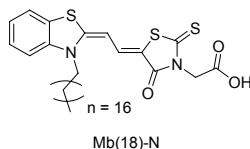


Figure 5. Merocyanine dye.

Organic dyes have some advantages over conventional ruthenium based chromophores as photosensitizers. They exhibit high molar extinction coefficients and are easily modified due to relatively short synthetic routes. The high extinction coefficients of the organic dyes are suitable for the thin TiO₂ films required in solid state devices where mass transport and insufficiently pore filling limit the photovoltaic performance.¹⁹

In recent years, a great deal of research aiming at finding highly efficient, stable organic sensitizers has been performed. A number of coumarin,²⁰ indoline,²¹ and triphenylamine²² based organic sensitizers (figure 6), have been intensively investigated and some of them have reached efficiencies in the range of 3-8%.^{9,20c,21,22b-d,23} All these sensitizers are efficient and represent one strategy in developing new chromophores, namely, reaching as high efficiency as possible and dealing with possible stability issues of the chromophore at a later stage. Perylenes represent the second strategy, starting from highly photo-

¹⁷ Sayama, K.; Hara, K.; Mori, N.; Satsuki, M.; Suga, S.; Tsukagoshi, S.; Abe, Y.; Sugihara, H.; Arakawa, H. *Chem. Commun.*, **2000**, 1173-1174.

¹⁸ (a) Tsubomura, H.; Mastumura, M.; Nomura, Y.; Amamiya, T. *Nature*, **1976**, *261*, 402-403. (b) Rao, T. N.; Bahadur, L. *J. Electrochem. Soc.*, **1997**, *144*, 179-185. (c) Nasr, C.; Liu, D.; Hotchandani, S.; Kamat, P.V. *J. Phys. Chem.*, **1996**, *100*, 11054-11061. (d) Ferrere, S.; Zaban, A.; Gregg, B.A. *J. Phys. Chem. B*, **1997**, *101*, 4490-4493. (e) Sayama, K.; Sugino, M.; Sugihara, H.; Abe, Y.; Arakawa, H. *Chem. Lett.*, **1998**, 753-754.

¹⁹ Schmidt-Mende, L.; Bach, U.; Humphry-Baker, R.; Horiuchi, T.; Miura, H.; Ito, S.; Uchida, S.; Grätzel, M. *Adv. Mater.* **2005**, *17*, 813-815.

²⁰ (a) Hara, K.; Sayama, K.; Ohga, Y.; Shinpo, A.; Suga, S.; Arakawa, H. *Chem. Commun.* **2001**, 569-570. (b) Hara, K.; Sato, T.; Katoh, R.; Furube, A.; Ohga, Y.; Shinpo, A.; Suga, S.; Sayama, K.; Sugihara, H.; Arakawa, H. *J. Phys. Chem. B* **2003**, *107*, 597-606. (c) Wang, Z.S.; Cui, Y.; Hara, K.; Dan-oh, Y.; Kasada, C.; Shinpo, A. *Adv. Mater.* **2007**, *19*, 1138-1141.

²¹ (a) Horiuchi, T.; Miura, H.; Sumioka, K.; Uchida, S. *J. Am. Chem. Soc.* **2004**, *126*, 12218-12219. (b) Horiuchi, T.; Miura, H.; Uchida, S. *Chem. Commun.* **2003**, 3036-3037.

²² (a) Velusamy, M.; Thomas, K. R. J.; Lin, J. T.; Hsu, Y. C.; Ho, K. C., *Org. Lett.* **2005**, *7*, 1899-1902. (b) Kitamura, T.; Ikeda, M.; Shigaki, K.; Inoue, T.; Andersson, N.A.; Ai, X.; Lian, T.; Yanagida, S. *Chem. Mater.* **2004**, *16*, 1806-1812. (c) Jung, I.; Lee, J.K.; Song, K.H.; Song, K.; Kang, S.O.; Ko, J. *J. Org. Chem.* **2007**, *72*, 3652-3658. (d) Liang, M.; Xu, W.; Cai, F.; Chen, P.; Peng, B.; Chen, J.; Li, Z. *J. Phys. Chem.* **2007**, *111*, 4465-4472.

²³ Koumura, N.; Wang, Z.S.; Mori, S.; Miyashita, M.; Suzuki, E.; Hara, K. *J. Am. Chem. Soc.* **2006**, *128*, 14256-14257. Our contributions are not included here.

stable sensitizers, dealing with the efficiency issue by introducing different substituents on the perylene framework. The perylenes have so far reached efficiencies around 2.3%.²⁴

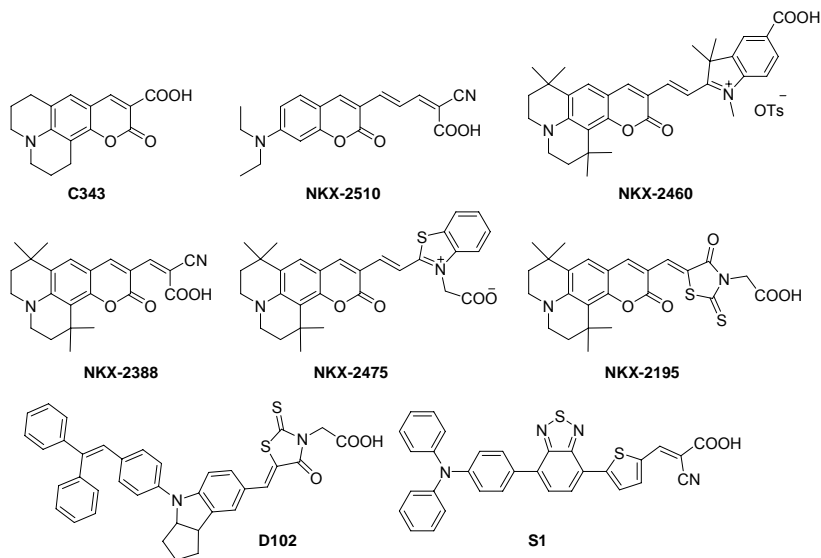


Figure 6. Examples of organic dyes.

The organic sensitizers can be divided in three major parts; donor, linker and acceptor components. Excitation by light should induce an intramolecular charge separation of the donor and acceptor moieties of the chromophore, i.e. a pronounced push-pull effect. The linker should increase the redshift in the absorption spectrum, and be rigid for long term stability. As one can imagine the number of combinations of different donors, linkers and acceptors is huge, and a trial and error strategy would be both time consuming and expensive.

²⁴ Example of perylene sensitizers: (a) Shibano, Y.; Umeyama, T.; Matano, Y.; Imahori, H. *Org. Lett.* **2007**, *9*, 1971-1974. (b) Edvinsson, T.; Li, C.; Pschirer, N.; Schöneboom, J.; Eickemeyer, F.; Sens, R.; Boschloo, G.; Herrman, A.; Müllen, K.; Hagfeldt, A. *J. Phys. Chem. C* **2007**, *111*, 15137-15140.

1.2.3. Solid State Dye Sensitized Solar Cells

An alternative to the iodide/triiodide redox system is an amorphous organic hole conductor, such as spiro-OMeTAD (figure 7). The replacement of the liquid electrolyte with a solid state charge carrier is advantageous when it comes to long-term stability problems of the volatile liquid electrolyte.¹⁹

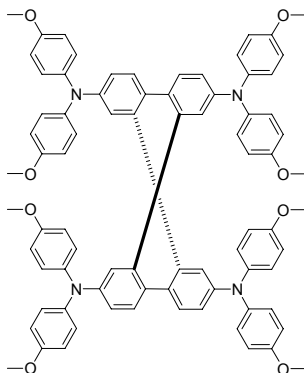


Figure 7. Structure of spiro-OMeTAD.

1.3. The Aim of This Thesis

The aim of this work was to prepare new efficient organic chromophores for dye sensitized solar cells and to investigate the fundamental requirements for such chromophores. During this work a strategy to obtain an efficient sensitizer was developed, where the donor, linker or acceptor moieties were alternated independently, tuning the HOMO and LUMO energy levels of the chromophores. Using our first reported dye as internal standard, the contributions of different donor, linker and acceptor groups can be used to attain a “HOMO and LUMO energy level library”.

2. Donor-Linker-Acceptor Systems: Synthesis of a Triphenylamine Based Dye.

(Paper I)

2.1. Introduction

Dividing the organic sensitizer in three parts; donor, linker and acceptor, is a convenient method to systematise the sensitizers. There are several basic criteria that an efficient sensitizer should fulfill, and these criteria can be used when designing a new chromophore. First of all, light excitation should be associated with vectorial electron flow from the light harvesting moiety of the dye, i.e. the donor and the linker, towards the proximity of the semiconductor, i.e. the acceptor/anchoring group of the dye. This can be seen as the HOMO is located over the donor and the linker, while the LUMO is located over the acceptor, i.e. a pronounced push-pull effect. Second, the HOMO potential of the dye should be sufficiently positive compared to the electrolyte redox potential for efficient dye regeneration.¹⁴ Third, the LUMO potential of the dye should be sufficiently negative to match the potential of the conduction band edge of the TiO₂. Fourth, a strong conjugation and electronic coupling across the donor and the acceptor to ensure high electron transfer rates. Finally, to obtain a dye with efficient photocurrent generation, π -stacked aggregation on the semiconductor should be avoided.²⁵ Aggregation may lead to intermolecular quenching or molecules residing in the system not functionally attached to the semiconductor surface and thus acting as filters.

2.1.1. Triarylamine in Conducting Materials

Due to the electron-donating nature of triarylaminines, they have been widely used as hole-transporting materials for a number of applications, such as xerography, organic field-effect transistors, photorefractive systems, light emitting diodes etc.²⁶ Long-lived charge separate states and multiphoton absorbing abilities have been reported for some of these triarylamine based

²⁵ Wang, Z. S.; Li, F. Y.; Huang, C. H.; Wang, L.; Wei, M.; Jin, L. P.; Li, N. Q., *J. Phys. Chem. B* **2000**, *104*, 9676-9682.

²⁶ (a) Fchetti, A.; Yoon, M.-H.; Marks, T J. *Adv. Mater.* **2005**, *17*, 1705-1708. (b) Li, H.; Lambert, C. *Chem. Eur. J.* **2006**, *12*, 1144-1155. (c) Cho, J.-S.; Kimoto, A.; Higuchi, M.; Yamamoto, K. *Macromol. Chem. Phys.* **2005**, *206*, 635-641. (d) Thomas K. R. J.; Lin, J. T.; Tao, Y.-T.; Ko, C.-W. *J. Am. Chem. Soc.* **2001**, *123*, 9404-9411. (e) Spraul, B.K.; Suresh, S.; Sassa, T.; Herranz M.A.; Echegoyen, L.; Wada, T.; Perahia, D.; Smith Jr., D.W. *Tetrahedron lett.* **2004**, *45*, 3253-3256.

materials.²⁷ In photovoltaic cells the interest of using triarylamine based sensitizers has increased in recent years.²² Studies of ruthenium complexes with triphenylamine as electron donor moiety have shown interesting results promising for DSC applications.²⁸ However, organic sensitizers with triphenylamine (TPA) donor moieties published when this project started (figure 8), included in some cases relatively long synthetic procedures which would have yielded high production costs and their efficiencies in the DSC was relatively low ($\eta_{\max} = 3.8\text{-}5.5\%$) compared to for instance some indoline sensitizers.^{21,22}

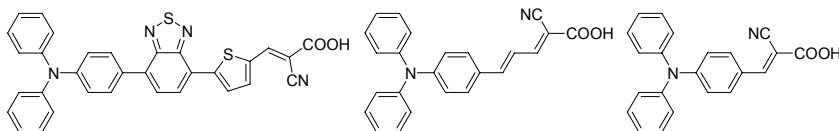


Figure 8. Examples of TPA sensitizers published at the start of the project.

At this point in time, the number of TPA based sensitizers has increased and modifications have been made both at the TPA moiety, with different substituents and at the linker unit, where different π -conjugated systems have been investigated.^{9,22,29} The TPA moiety is non-planar and can suppress aggregation due to the disturbance of the π - π stacking.

2.1.2. Thiophenes as π -Conjugated Linker

Expansion of the π -conjugated C=C backbone to extend the absorption spectrum and broaden it to the red region, is one way to decrease the HOMO/LUMO energy level differences and thereby increase the solar cell performance. This would, however, complicate the synthetic procedure and affect the stability of the dye due to photoinduced *trans* to *cis* isomerisation.³⁰ The introduction of different π -conjugated ring moieties, such as thiophene, benzene or pyrrole is an elegant way of extending the π -conjugated system without affecting the stability of the dye.³¹ In 2003 Hara et al. reported a series of coumarine dyes with different linker units (figure 9).³¹

²⁷ (a) Bonhote, P.; Moser, J. E.; Humphry-Baker, R.; Vlachopoulos, N.; Zakeeruddin, S.; Walder, L.; Grätzel, M. *J. Am. Chem. Soc.* **1999**, *121*, 1324-1336. (b) Belfield, K.D.; Schafer, K. J.; Mouard, W.; Reinhardt, B. A.; *J. Org. Chem.* **2000**, *65*, 4475-4481.

²⁸ (a) Moser, J. E., *Nature Mater.* **2005**, *4*, 723-724. (b) Kitamura, T.; Ikeda, M.; Shigaki, K.; Inoue, T.; Anderson, N. A.; Ai, X.; Lian, T.; Yanagida, S., *Chem. Mater.* **2004**, *16*, 1806-1812.

²⁹ Our contributions are not included here.

³⁰ Lequan, M.; Lequan, R.M.; Chane-Ching, K.; Callier, A. C. *Adv. Mater. Opt. Electron.* **1992**, *1*, 243-248.

³¹ Hara, K.; Kurashige, M.; Dan-oh, Y.; Kasada, C.; Shinpo, A.; Suga, S.; Sayama, K.; Arakawa, H., *New J. Chem.* **2003**, *27*, 783-785.

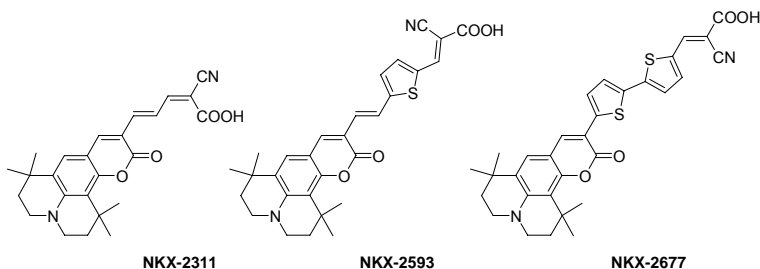


Figure 9. π -conjugated extension by thiophene introduction in the linker.

By introducing a thiophene in the linker, the absorption spectrum is indeed broadened toward the red region when the dyes are adsorbed on the surface of TiO_2 , leading to an increase of the photocurrent. **NKX-2593** and **NKX-2677** both show efficiencies over 7% and have almost identical absorption spectra. From a synthetic point of view, **NKX-2593** requires a slightly shorter synthetic route than **NKX-2677** to obtain approximately the same efficiency.

2.1.3. Cyanoacrylic Acid as Acceptor and Anchoring Group.

The carboxylic acid group is by far the most employed group for attachment of the sensitizers to the semiconductor surface. The binding modes (figure 10) have been investigated by Galoppini and co-workers.³²

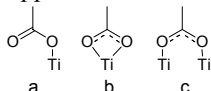


Figure 10. Main binding modes of carboxylate group to TiO_2 , a) monodentate, b) bidentate chelating, c) bridging bidentate.

When it comes to the slightly wider term acceptor groups, cyanoacrylic acid is by far most commonly used due to its strong electronic withdrawing properties. There is a number of different acceptor groups reported and some show promising results (figure 11).^{20,21,33} In some cases, the ending of the linker and the beginning of acceptor lie in the eye of the beholder, since the increased conjugation that some acceptor groups provides will broaden the absorption spectra. However, in this thesis a synthetic point of view will be used to differentiate the linker and the acceptor depending on the reactants used.

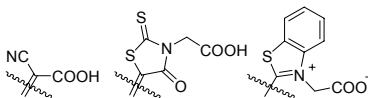


Figure 11. Examples of different acceptor groups

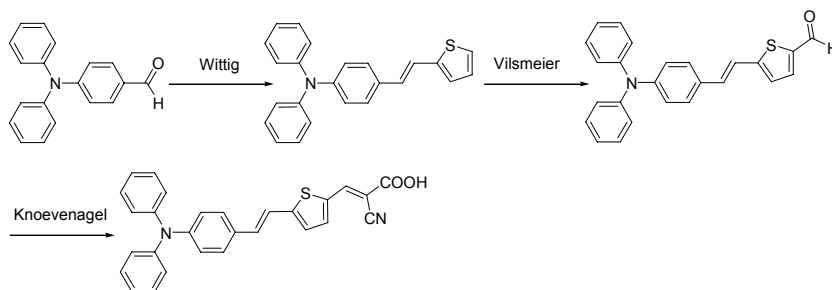
³² Rochford, J.; Chu, D.; Hagfeldt, A.; Galoppini, E. *J. Am. Chem. Soc.* **2006**, *129*, 4655-4665.

³³ Otaka, H.; Kira, M.; Yano, K.; Ito, S.; Mitekura, H.; Kawato, T.; Matsui, F. *J. Photochem. Photobiol. A*, **2004**, *164*, 67-73.

2.1.4. Aim of the Study and Synthetic Strategy

We designed an organic chromophore based on triphenylamine as the donor group, with a thiophene linker and a cyanoacrylic acid moiety as acceptor/anchor group that would be an interesting starting point for further modifications (scheme 1). The synthetic strategy included well-known methodology, such as Wittig,³⁴ Vilsmeier and Knoevenagel reactions.

Scheme 1. Synthetic strategy of TPA based dye.



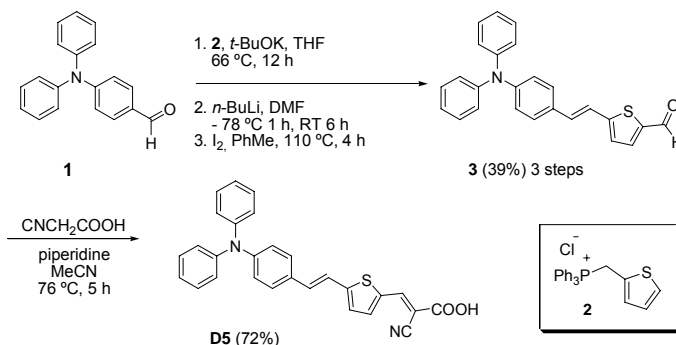
2.2. TPA Based Dye (**D5**) for DSCs

2.2.1. Synthesis of **D5**

For the synthesis of TPA based dye **D5**, 2-thiophenemethylphosphine **2** was coupled to commercially available 4-(diphenylamino)benzaldehyde **1** accordingly to the Wittig reaction (scheme 2).³⁴ The Wittig reagent **2** was prepared from 2-thiophenemethanol in a two-step procedure, in almost quantitative yield.^{34b} Since the Wittig reagent would yield a stabilized ylid, whose anion is stabilized by further conjugation, the reaction should be *E*-selective. However, severe overlapping in the aromatic region in the ¹H-NMR spectrum, did not allow the determination of the *E-Z* selectivity. Formylation of the thiophene moiety by the Vilsmeier reaction proved to be a problem and a number of different formylated species was monitored in the ¹H-NMR spectrum. Instead the use of *n*-BuLi in DMF at -78 °C proved to be successful and yielded only the 2-formylated thiophene. In the ¹H-NMR however, we could now observe the existence of both the *cis* and *trans* isomers, hence *cis* to *trans* isomerisation using I₂ was performed, yielding the desired product **3**. The final step in the synthesis was condensation of the aldehyde according to the Knoevenagel protocol in presence of piperidine.

³⁴ (a) Wittig, G. *J. Organomet. Chem* **1975**, *100*, 279. (b) Hu, Z.Y.; Fort, A.; Barzoukas, M.; Jen, A.K.Y.; Barlow, S.; Marder, S.R. *J. Phys. Chem. B* **2004**, *108*, 8626-8630.

Scheme 2. Synthetic route to **D5**



2.2.2. Solar Cell Performance of **D5**

UV-vis and fluorescence spectra of **D5** in acetonitrile showed two absorption bands with absorption maxima at 476 nm and 300 nm (figure 12).

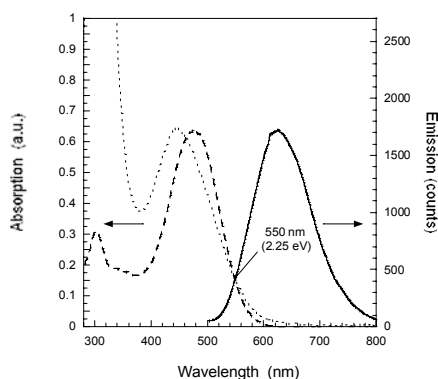


Figure 12. Absorption (---) and emission (—) of **D5** in MeCN compared with the absorption spectrum of **D5** attached to TiO_2 (.....).³⁵

When the dye was attached to the TiO_2 surface, a blueshift of the absorption maximum from 476 nm to 444 nm was found. The blueshift originates from the interaction with TiO_2 . In methanol the same blueshift occurred, indicating that the blueshift arises from polar interaction and/or deprotonation. However, when adding acetic acid in methanol, a redshift to 474 nm was observed, revealing that the blueshift mainly originates from deprotonation. Cyclic voltammetry (CV) and square wave voltammetry (SWV) were employed to measure the oxidation and reduction potentials of **D5** (figure 13). The oxidation potential was determined to 450 mV and the reduction potential to -

³⁵ Absorption and emission measurements performed by Tomas Edvinsson and Tannia Marinado.

1550 mV vs. Fc/Fc^+ (1080 mV and -920 mV vs. NHE, respectively), which is energetically favorable for regeneration from the electrolyte, i.e. the iodide/triiodide redox couple. Estimating the HOMO energy level in MeCN from the formal oxidation potential and adding the zeroth-zeroth energy $\Delta E_{0-0} = 2.25$ eV (taken from figure 12) we arrive at -1.17 V vs. NHE for the LUMO. This is well above the conduction band level of TiO_2 at approximately -0.36 V vs. NHE.

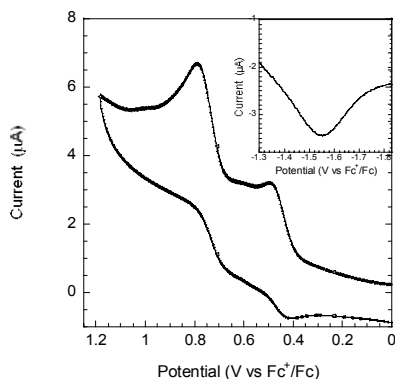


Figure 13. Cyclic voltammogram of the oxidation behaviour and square wave voltammogram (inset) of the reduction.³⁶

The electronic redistribution between the HOMO and LUMO, illustrated in figure 14, indicates a pronounced intramolecular charge separation, i.e. a strong push-pull effect. The LUMO orientation over the acceptor group will favor electron injection assuming similar molecular orbital distribution when the dye is attached to the semiconductor surface.

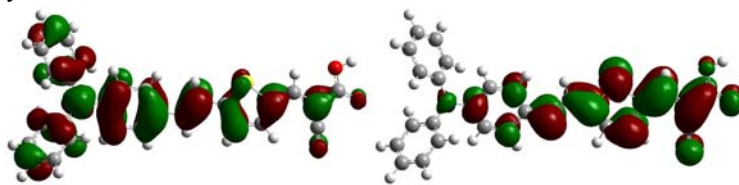


Figure 14. HOMO and LUMO distribution calculated with TD-DFT on a B3LYP/6-31 + G(d) level.³⁷

IPCE measurement of **D5** shows a peak value of 85% at 400 nm and 70-65% at the plateau between 450-600 nm (figure 15). This indicates high light harvesting ability for **D5**, and the photovoltaic performance was promising

³⁶ CV and SWV measurements performed by Tomas Edvinsson.

³⁷ TD-DFT calculations performed by Tomas Edvinsson.

with an overall solar-to-electric conversion efficiency (η) of 5.1%, compared to **N719** (chapter 1) which under the same conditions gave $\eta = 6\%$.

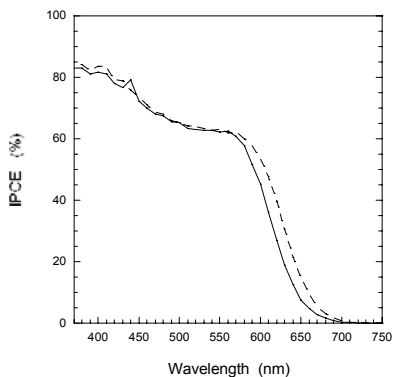


Figure 15. IPCE spectra for dye sensitized TiO_2 solar cells with (---) and without scattering layer (—). The electrolyte was 0.6 M TBAI, 0.1 M LiI, 0.05 M I_2 and 0.5 M 4-TBP in MeCN.³⁸

Analysis of the experimental and theoretical data revealed optimization possibilities. By putting the HOMO and LUMO energy levels of the chromophore in a diagram compared to the conduction band of the semiconductor and the redox potential of the electrolyte, it becomes obvious that the HOMO and LUMO energy level gap can be decreased to gain photovoltaic current (figure 16).

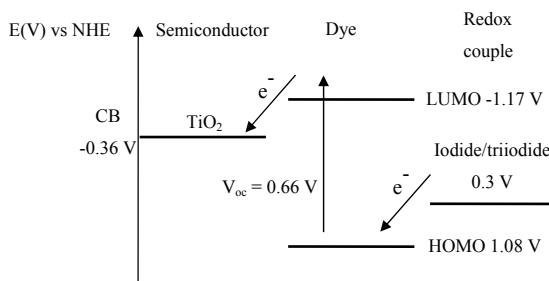


Figure 16. Energy level diagram of the DSC

³⁸ IPCE measurement performed by Tomas Edvinsson and Tannia Marinado.

2.3. Conclusions

We have designed and synthesized an organic sensitizer, **D5**, for DSC applications. The sensitizers can be prepared in moderate yield via a short synthetic route using well known methodology. The overall solar-to-electric conversion efficiency was over 5%, compared to the conventional **N719** dye which gave 6% under the same conditions. This chromophore stands as a ground for further optimizations, where the absorption should be broadened and the HOMO and LUMO energy level gap should be decreased.

3. Linker Variation of TPA Based Chromophores: Synthesis of π -Conjugated Thiophene Dyes

(Paper II)

3.1. Introduction

Increased conjugation by linker modifications is one way to broaden the absorption spectra and hence decreasing the HOMO and LUMO energy level gap. However, there is a limit where the energy level potential of the HOMO becomes too low and the regeneration from the electrolyte, i.e. iodide/triiodide, is hindered.¹⁰ The limit for the LUMO energy level is not of the same importance since the conduction band potential of the semiconductor can be tuned by additives in the electrolyte.³⁹

3.1.1. Aim of the Study

By altering the linker moiety independent of the donor and the acceptor, we can screen the contributions of different linkers and attain a “HOMO and LUMO energy library” (figure 17). A series of chromophores, **L0-L4**, with increasing linker conjugation was prepared. The dye **L2** is the same as **D5** in chapter 2. This screening strategy helps us to optimize the TiO₂ – dye – iodide/triiodide system in terms of balance between photovoltage, driving forces and spectral response. In this series the double bond consisting chromophores are all *trans* isomers which have higher photostability properties.³⁰

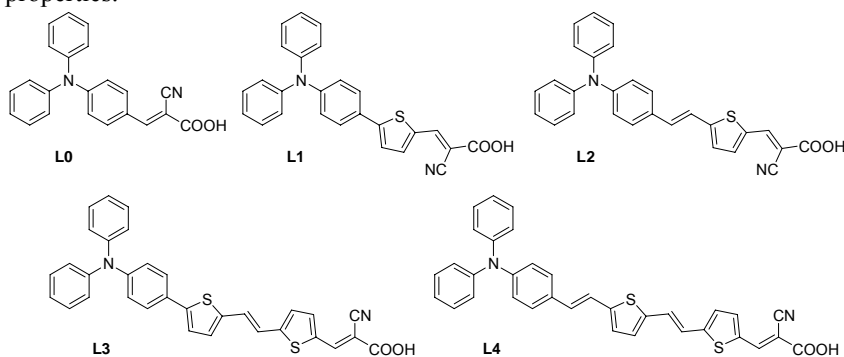


Figure 17. Structures of the chromophores.

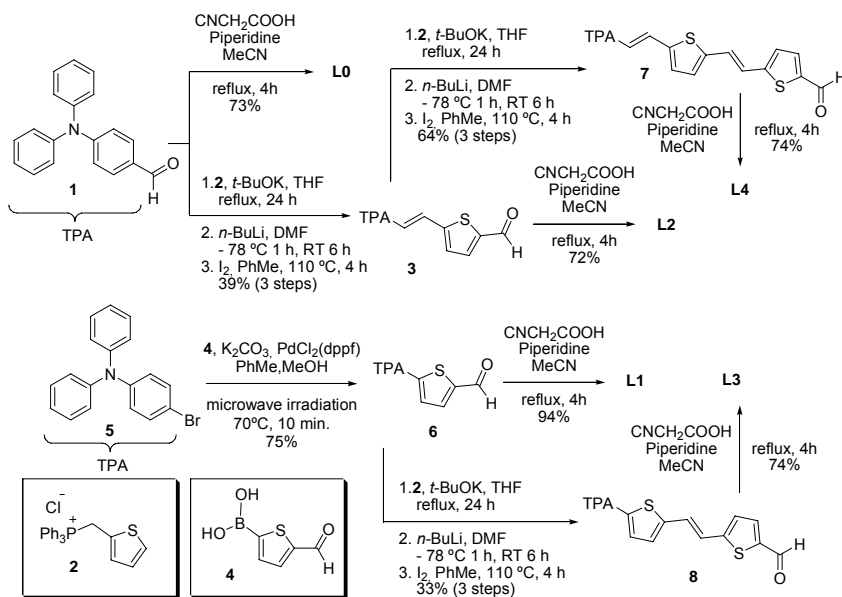
³⁹ Redmond, G.; Fitzmaurice, D. *J. Phys. Chem.* **1993**, *97*, 1426-1430.

3.2. Extended π -Conjugation in TPA Based Dyes

3.2.1. Synthesis of Linker Series

To extend the linker π -conjugation, a Suzuki coupling reaction⁴⁰ (**L1**) and/or a Wittig reaction³⁴ (**L2**, **L3** and **L4**) were employed (scheme 3). The Suzuki coupling reaction was performed with unprotected 5-formyl-2-thiopheneboronic acid **4** and 4-(diphenylamino)bromobenzene **5** under microwave irradiation to directly yield aldehyde **6**, necessary for further reactions, i.e. Knoevenagel reaction or Wittig reaction.⁴¹ In the cases of linker extension by the Wittig reaction, formylation of the thiophene moiety using *n*-BuLi and DMF was applied. As described in chapter 2, ¹H-NMR revealed the existence of both the *cis* and *trans* isomers, hence *cis* to *trans* isomerisation using I₂ was performed which yielded the desired *trans* products (**3**, **7** and **8**). The final step in the synthesis of these chromophores was again condensation of the aldehydes with cyanoacetic acid according to the Knoevenagel protocol in presence of piperidine.

Scheme 3. Synthesis of linker series



⁴⁰ Suzuki, A. *J. Organomet. Chem* **1999**, 576, 147-168.

⁴¹ Melucci, M.; Barbarella, G.; Zambianchi, M.; Di Pietro, P.; Bongini, A. *J. Org. Chem.* **2004**, 69, 4821-4828.

3.2.2. Solar Cell Performance of Linker Series

As expected, a systematic redshift in the absorption maximum with increasing conjugation was observed (figure 18, left). To exclude the absorption maximum difference due to protonation/deprotonation as discussed in chapter 2, TBAOH was added to the dye solutions. Upon adsorption onto the semiconductor, TiO₂, the dye spectra were broadened (figure 18, right). The absorption shoulder on the low energy side was extended with increased linker conjugation, hence the spectral behavior of the dye series was as proposed. The emission spectra also showed an equivalent redshift upon increasing linker conjugation (table 1). The oxidation potentials of the dyes in acetonitrile were determined by differential pulse voltammetry and are listed in table 1. Increased linker conjugation length indeed resulted in less positive oxidation potentials and the estimated LUMO potentials calculated from ($E_{ox}-E_{0-0}$), were sufficiently more negative than the TiO₂ conduction band edge for all five dyes (table 1).

Table 1. Absorption, emission and electrochemical properties.⁴²

Dye	Abs _{max} [nm] ^a	ϵ [M ⁻¹ cm ⁻¹] ^b	Em _{max} [nm] ^c	E _(ox) [V] vs. NHE ^d	E ₀₋₀ [eV] ^e	E _{LUMO} [V] vs. NHE ^f
L0^g	373 ⁱ , 387 ⁱⁱ	36 000	509	1.37	2.90	-1.53
L1	404 ⁱ , 404 ⁱⁱ	25 000	548	1.21	2.64	-1.43
L2	427 ⁱ , 409 ⁱⁱ	38 000	594	1.13	2.48	-1.36
L3	445 ⁱ , 412 ⁱⁱ	49 000	621	1.07	2.38	-1.32
L4	463 ⁱ , 415 ⁱⁱ	62 000	644	1.01	2.35	-1.34

^aAbsorption of the deprotonated dyes in MeCN solutionⁱ and adsorbed onto TiO₂ⁱⁱ. ^bAbsorption coefficients determined in THF solution. ^cEmission maximum of the deprotonated dyes in acetonitrile, excited at absorption maximum. ^dThe ground state oxidation potential (first oxidation peak) of the dyes were measured with Differential Pulse Voltammetry, DVP, under the following conditions: 0.1 M tetrabutylammonium hexafluorophosphate, TBA(PF₆) in acetonitrile, a Pt working electrode, a silver counter electrode and the reference electrode was a silver wire calibrated with Ferrocene/Ferrocenium (Fc/Fc⁺) as an internal reference. ^eThe 0-0 transition energy was estimated from the intersection of normalized absorption and emission curves from solution measurements.^f The estimated LUMO position from addition of the estimated 0-0 transition energy to the ground state oxidation potential vs. NHE.^g Previously studied by Kitamura et al.²²

⁴² Absorption, emission and electrochemical measurements performed by Tannia Marinado.

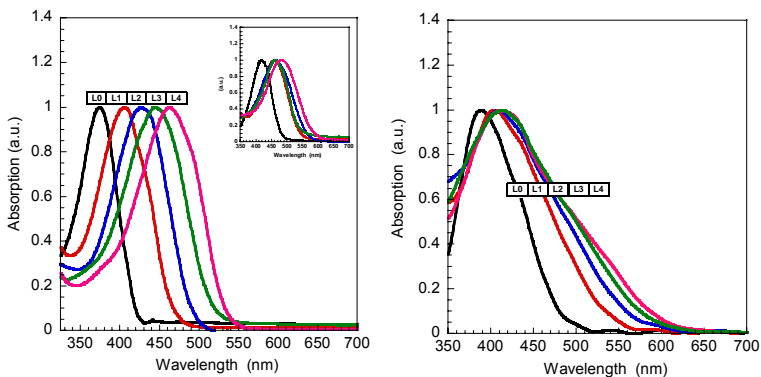


Figure 18. (left) Normalized absorption spectra of the L0-L4 dyes in acetonitrile solution upon addition of TBAOH. Inset: Normalized absorption spectra of the L0-L4 dyes in a plain acetonitrile solution. (right) Normalized absorption spectra of the L0-L4 dyes adsorbed onto TiO_2 .⁴²

Computed HOMO and LUMO of **L1** and **L4** are depicted in figure 19. The general characters of the orbitals are independent of the linker length. The HOMO is of π -characteristics and is delocalized over the entire molecule, including the phenyl groups of the amino nitrogen. In the LUMO, which also has π -character, there is essentially no contribution from the amino phenyl groups, and the electron density has been shifted towards the acceptor group of the chromophores. This supports the supposed push-pull characteristics of these chromophores.

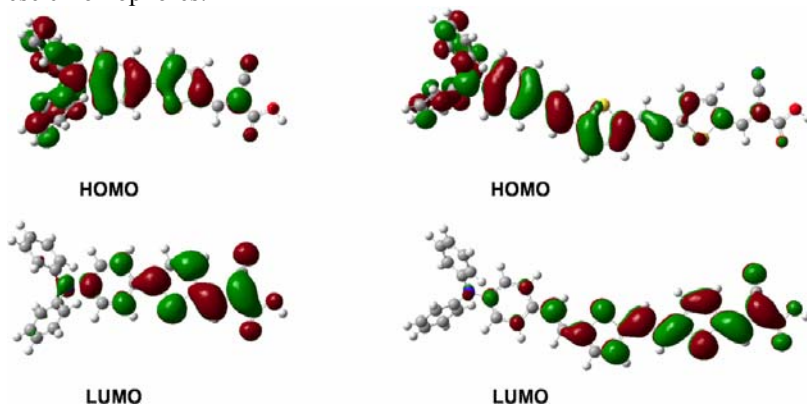


Figure 19. Computed isodensity surfaces of HOMO and LUMO of the L1 and L4 chromophores.⁴³

Solar cell performances were measured using thin TiO_2 films ($\sim 3 \mu\text{m}$). The IPCE (figure 20) show low energy onsets that correlate well with the E_{0-0} of

⁴³ Isodensity calculations performed by Tore Brinck.

the individual dyes. **L0** and **L1** showed high IPCE (75%) but have narrow spectra which give lower photocurrents, in contrast to **L3** and **L4** which displayed broad spectra but low IPCE. **L2** (**D5** in chapter 2) showed a broad spectra with reasonable high IPCE. As a comparison the **N719** dye was also included; **N719** yields low and broad IPCE when adsorbed on these thin semiconductor films. The trend with lower IPCE peak values with increasing linker conjugation probably arised from the dye load. The dye load decreased as the size of the dye increased (table 2). Assuming a monolayer on the semiconductor surface, a larger dye would have a larger footprint (excluded volume) and hence result in lower dye load. Considering the light harvesting efficiency, the relatively lower dye load of the larger dyes would be compensated by their higher extinction coefficients. The lower IPCE for **L3** and **L4** dyes could be caused by poor injection efficiency, possibly due to unfavorable binding or orientation of these dyes onto the TiO₂ surface.

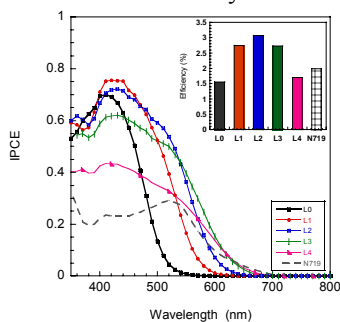


Figure 20. Spectra of monochromatic IPCE for DSC based on **L0-L4** and **N719**.
Inset: Solar cell efficiency based on respective dye.⁴⁴

The photovoltaic performances of solar cells based on the different chromophores **L0-L4** and **N719** are summarized in table 2 and depicted in figure 17. Dark current measurements indicated an increasing electron recombination from the semiconductor to the electrolyte as the linker conjugation increases (appendix II). Concerning the observed trend in overall efficiencies, organic dyes, **L1-L3**, with comparable spectral properties were performing better than **N719** due to higher extinction coefficients.

⁴⁴ IPCE and solar cell performances measurements performed by Tannia Marinado

Table 2. Current and voltage characteristics of DSCs (3 μm thick WE) based on the **L0-L4**.⁴⁵

Dye	V _{oc} [mV]	η [%]	ff	J _{sc} [mA/cm ²]	Dye load ^a [μmol/cm ³]	Relative amount ^b
L0	735	1.55	0.73	2.89	227	1
L1	735	2.75	0.69	5.42	313	1.38
L2	710	3.08	0.68	6.42	264	1.16
L3	635	2.73	0.66	6.55	202	0.89
L4	580	1.70	0.64	4.56	133	0.59
N719	735	1.99	0.75	3.63	-	-

Photovoltaic performance under AM 1.5 irradiation of DSCs based on **L0-L4** and **N719**, respectively, based on 0.6M TBAI, 0.1M LiI, 0.05M I₂, 0.5 M 4-TBP electrolyte in acetonitrile. J_{sc} is the short-circuit photocurrent density; V_{oc} is the open-circuit voltage, ff is the fill factor and η the power conversion efficiency. ^aThe dye loads are calculated from absorbance data of the sensitized TiO₂ electrodes. ^bThe relative amount is calculated in reference to dye **L0**.

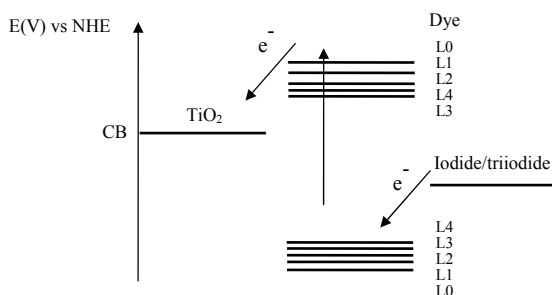


Figure 21. Schematic energy level diagram of the DSC and the linker series.

3.3. Conclusions

Chromophores **L0-L4** show satisfactory efficiencies on thin TiO₂ films (3 μm), and are therefore suitable for future solid state devices where thin semiconductor films are required. By increasing the π-conjugation the HOMO and LUMO energy levels were tuned. Even though all dyes fulfill the energetic criteria for DSC (figure 21) the longer linker chromophores showed pronounced losses, however. The longer linker conjugation leads to increased spectral response but increases recombination of electrons to the triiodide. The lower IPCEs obtained for the longer **L3** and **L4** dyes could be due to the

⁴⁵ Current and voltage characteristics measurements performed by Tannia Marinado.

specific nature of the dyes (size/structure, orientation on the surface and chemical properties). To support this assumption, further investigations have to be done. Solar cells based on **L2** (**D5** in chapter 2) yielded the highest efficiency. The **L2** chromophore thus shows the optimal properties, considering energy levels, dye load and the orientation on the semiconductor surface.

4. Acceptor Group Modification and Linker Variation of TPA Based Chromophores: Synthesis of Rhodanine-3-acetic Acid Dyes

(Paper III)

4.1. Introduction

The first efficient organic sensitizer (**Mb(18)-N**)¹⁷ (described in chapter 1), had the rhodanine-3-acetic acid as acceptor group. Since then, as mentioned in chapter 1 and 2, Hara et al. and Horiuchi et al. investigated coumarin and indoline based chromophores, using rhodanine-3-acetic acid as acceptor groups, which gave promising results also in the solid state solar cells.^{20, 21} In 2007 Liang et al. reported a TPA based chromophore with rhodanine-3-acetic acid as acceptor group.⁴⁶ However, this acceptor group has not yet been properly compared with cyanoacrylic acid, in terms of HOMO and LUMO energy level contributions.

4.1.1. Aim of the Study and Synthetic Strategy

In order to investigate the TPA donor based chromophores with a broadening of the absorption spectra by varying the π -conjugation of the linker, we designed three chromophores with rhodanine-3-acetic acid as acceptor group (figure 22). With the earlier study (chapter 3) in mind, we focused on the three shortest linkers (**L0**, **L1** and **L2**), which did not have dye load and recombination problems. The same synthetic route was used except from the last step where rhodanine-3-acetic acid was coupled to the chromophore according to the Knoevenagel reaction.

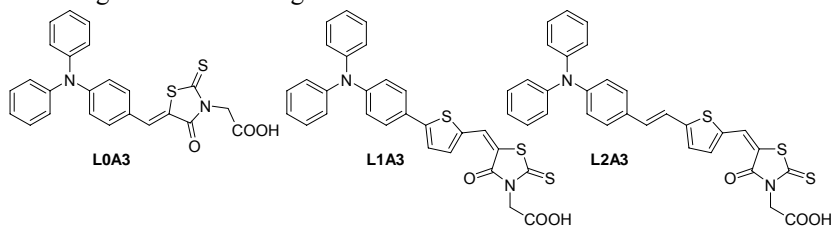


Figure 22. Structures of the chromophores

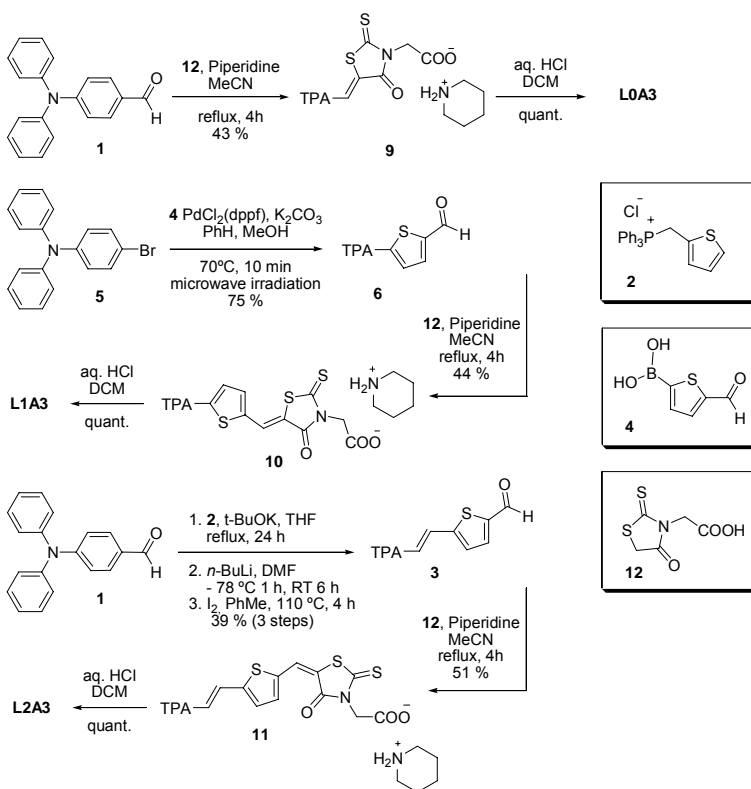
⁴⁶ Liang, M. X., W.; Cai, F.; Chen, P.; Peng, B.; Chen, J.; Li, Z. *J. Phys. Chem. C* **2007**, *111*, 4465-4472.

4.2. Acceptor Group Modification of Chromophores for DSC Applications.

4.2.1. Synthesis of Linker-Acceptor Series

The synthetic routes are depicted in scheme 4. When using a catalytic amount of piperidine in the Knoevenagel reactions the purification of the products was difficult. However, by using stoichiometric amounts of piperidine, the product precipitated upon cooling and could be filtered off (**9**, **10** and **11**). The precipitate was dissolved in DCM and washed with acidic water to yield the products.

Scheme 4. Synthesis of linker-acceptor series



4.2.2. Solar Cell Performance of Linker-Acceptor Series

For the three sensitizers **L0A3**, **L1A3** and **L2A3** a less positive HOMO energy level was obtained with increasing linker length in agreement with the expectations (table 3).

Table 3. Absorption, emission and electrochemical properties.⁴²

Dye	Abs _{max} [nm] ^a	ϵ [M ⁻¹ cm ⁻¹] ^b	Em _{max} [nm] ^a	E _{D/D+} [V] ^c vs. NHE	E _(o-o) [eV] ^d	E _(LUMO) [V] vs. NHE
L0A3	459 ⁱ , 438 ⁱⁱ	44 000	607	1.27	2.38	-1.11
L1A3	476 ⁱ , 459 ⁱⁱ	38 000	668	1.15	2.19	-1.04
L2A3	501 ⁱ , 469 ⁱⁱ	39 000	726	0.98	2.08	-1.10

However, the solar energy to electricity efficiency decreases with increasing linker length (table 4). This is surprising, since the HOMO energy level potential for this series is well above the potential for the redox couple.

Table 4. Current and voltage characteristics of DSCs.⁴⁵

Dye	V _{oc} (V)	J _{sc} (mA/cm ²)	ff	η (%)
L0A3	0.50	10.0	0.5	2.7
L1A3	0.44	10.5	0.5	2.3
L2A3	0.41	7.7	0.5	1.7

Recalling the trend for the linker in chapter 3, where the longest linkers had decreasing efficiencies due to larger footprints and hence less dye loads on the semiconductor surface, which leads to increasing recombination from the semiconductor to the electrolyte. To investigate the recombination and regeneration processes that may limit the photovoltaic performances, photoinduced absorption spectroscopy (PIA) was employed (appendix III).^{47,48} More specifically, the fate of the oxidized state of the dye in the absence and presence of an electron donor (I⁻) in the electrolyte was followed. PIA measurements confirmed that all three dyes can inject electrons in the conduction band of the TiO₂, i.e. they become oxidized after electronic excitation of the dye. For all three dyes the spectra of the oxidized dye were no longer visible in the presence of redox electrolyte, revealing that the regeneration of the oxidized dyes by iodide is not the limiting factor for the conversion efficiencies and thus not the reason of the different photovoltaic performances observed for the three dyes.

Turning to the HOMO and LUMO distributions over the dyes, depicted in figure 23, computational results show a poor extension of the LUMO on the rhodanine-3-acetic acid anchor group. Assuming that the orbital geometries are similar when the dyes are attached to TiO₂, this will result in poor electronic coupling for the electronic coupling for the electron injection from the dyes to the TiO₂ conduction band edge and hence lower overall photocurrents.

⁴⁷ Boschloo, G.; Hagfeldt, A. *Chem. Phys. Lett.* **2003**, 370, 381-386.

⁴⁸ Tannia Marinado performed the PIA measurements.

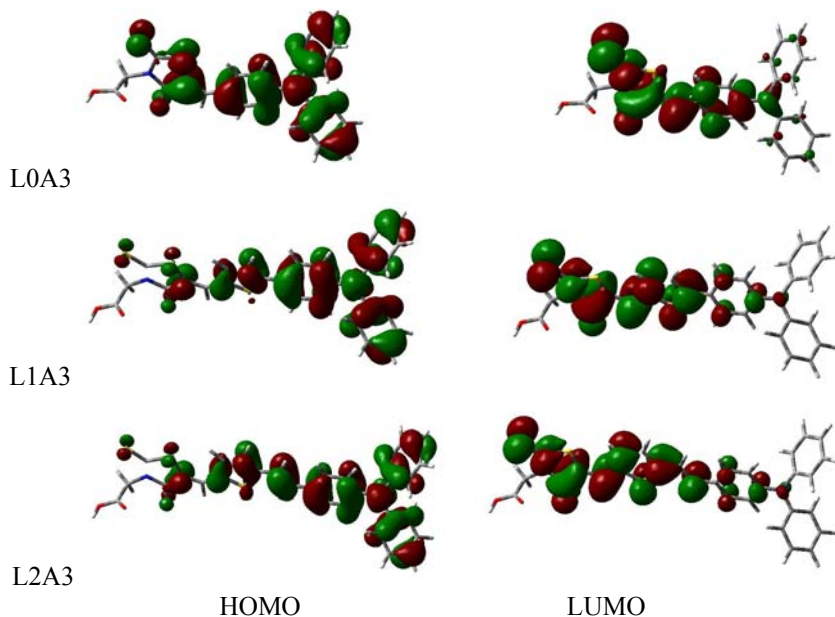


Figure 23. The frontier molecular orbitals of the HOMO (left) and LUMO (right) calculated with PCM-PBE1PBE/6-31+G(d) level. The electron redistribution of the orbitals shows a clear charge separation upon electronic excitation.⁴⁹

The IPCEs of the dyes **L0A3**, **L1A3** and **L2A3** are shown in figure 24. The same trend as was noted for the linker series in chapter 3, was observed, where the longer linker broadens the spectra but loses intensity.

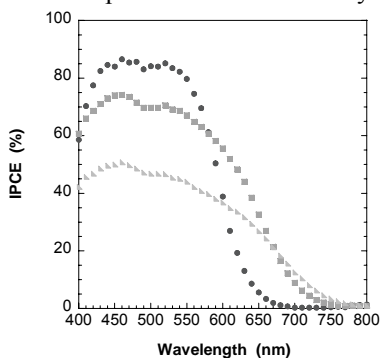


Figure 24. IPCE for DSC based on **L0A3** (●), **L1A3** (■) and **L2A3** (▸).⁵⁰

⁴⁹ Isodensity calculations performed by Tore Brinck.

⁵⁰ IPCE measurements performed by Tannia Marinado.

By comparing the three chromophores **L0A3**, **L1A3** and **L2A3** with their cyanoacetic acid analogues, one can clearly see the contribution to the HOMO and LUMO energy levels of the rhodanine-3-acetic acid acceptor group (figure 25).

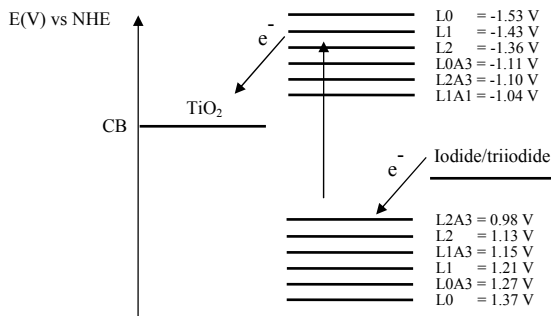


Figure 25. Schematic energy level diagram of the DSC and the linker series.

4.3. Conclusions

Rhodanine-3-acetic acid decreases the gap between the HOMO and LUMO energy levels, thus tuning the energy levels closer to the redox potential of the electrolyte and the conduction band of the semiconductor. However, the rhodanine-3-acetic acid acceptor group gives a poor extension of the LUMO towards the surface of the semiconductor. Hence the injection efficiencies are affected. This acceptor group has however, with promising results, been used in solid state devices, which have to be investigated before coming to a final verdict.^{20, 21}

5. Donor Variation of TPA Based Chromophores: Synthesis of Different TPA Based Donors

(Paper IV)

5.1. Introduction

A number of different donors have, as mentioned in chapter 1 and 2, been investigated, amongst them triphenylamine donors. However, the donors based on the TPA moiety with different modifications such as electron donating groups on the TPA framework are rare.⁴⁶ Hara et al. published in 2005 an interesting concept of putting two dimethylamine donor moieties in one chromophore.⁵¹ Oliva et al. recently reported the effect of different amine donors on the HOMO potential in oligothiophenes.⁵²

5.1.1. Aim of the Study and Synthetic Strategy

By adopting the double strategy for the TPA based donors and also introducing electron-donating substituents in the TPA framework, we designed a series of four different chromophores for DSC applications (figure 26).

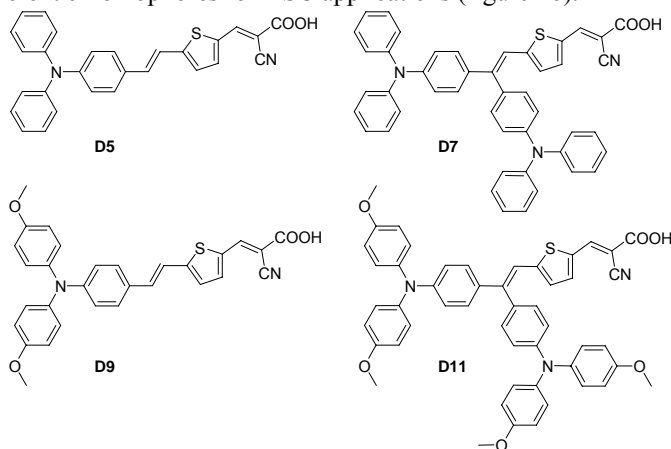


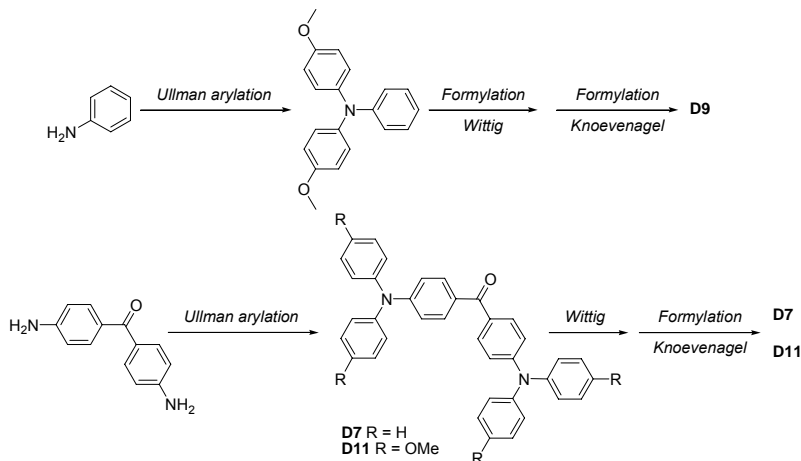
Figure 26. Structures of Chromophores.

⁵¹ Hara, K.; Sato, T.; Katoh, R.; Furube, A.; Yoshihara, T.; Murai, M.; Kurashige, M.; Ito, S.; Shinpo, A.; Suga, S.; Arakawa, H. *Adv. Funct. Mater.* **2005**, *15*, 246-252.

⁵² Oliva, M. M.; Casado, J.; Raposo, M. M. M.; Fonseca, A. M. C.; Hartmann, H.; Hernandez, V.; Navarrete, J. T. L.; *J. Org. Chem.* **2006**, *71*, 7509-7520.

The synthetic strategy used for the preparation of the chromophores (**D9**, **D7** and **D11**) follows the synthetic route of **D5** described in chapter 2. However, an Ullman arylation was performed to obtain the methoxy-substituted TPA and the di-triphenylamine based ketone (scheme 5).⁵³

Scheme 5. Synthetic strategy of TPA based dye.



5.2. Donor Modification of Chromophores for DSC Applications

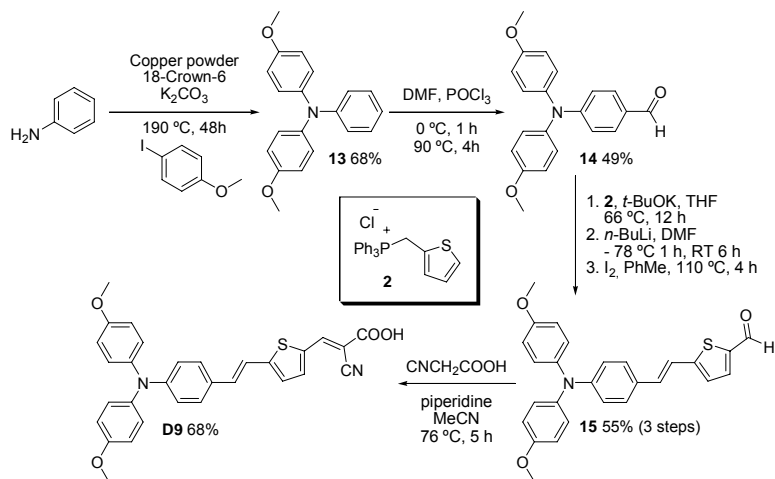
5.2.1. Synthesis of Linker Series

The synthetic route for **D9** is depicted in scheme 6 and that for **D7** and **D11** in scheme 7. By following the procedure reported by Plater et al. where aniline was functionalized by Ullman arylation, which gave the desired products in moderate yields. Purification was difficult due to the large excess of iodobenzene (**D7**) or iodoanisole (**D9** and **D11**) used.^{26e,53} The synthesis of **D9** includes a formylation of the phenyl moiety in **13**; this was achieved by the Vilsmeier reaction and yielded product **14**. From the formylated product **14**, the synthesis followed the same route as for the synthesis of **D5** (chapter 2). Wittig reaction of **16** with **2** was unsuccessful, probably due to steric hindrance. Instead the Horner-Wadsworth-Emmons reagent (alkylphosphonate ester **17**) was prepared. The phosphonate carbanion (from **17**) is more nucleophilic than the analogue ylide (from **2**). The Horner-Wadsworth-Emmons reaction was successful and the desired products were obtained in moderate to good yields.

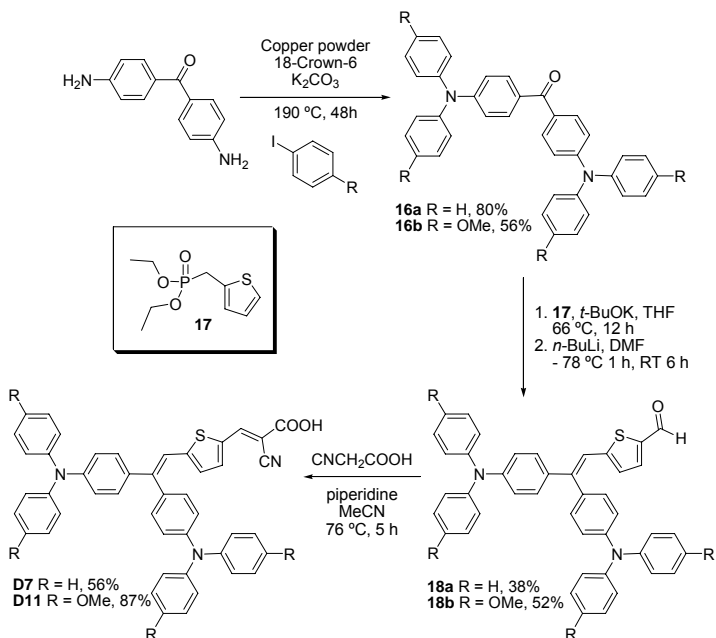
Formylation of the corresponding Horner-Wadsworth-Emmons product by *n*-BuLi and DMF yielded **18a** and **18b**. The final products were prepared according to the Knoevenagel reaction.

⁵³ Plater, M.J.; Jackson, T. *Tetrahedron*, **2003**, *59*, 4673-4685.

Scheme 6. Synthetic route to D9.



Scheme 7. Synthetic routes to D7 and D11.



5.2.2. Solar Cell Performance of Donor Series

The absorption spectra of the donor series (figure 27) show that the methoxy moiety of **D9** and **D11** redshift the absorption maximum, compared to the **D5** and **D7** chromophores. The absorption spectrum of **D11** was also broadened, this behavior is consistent with decreased gap between the HOMO and LUMO energy levels.

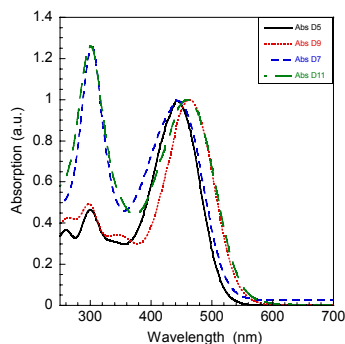


Figure 27. Absorption spectra of donor series.⁵⁴

The IPCE spectra are depicted in figure 28, and show a relatively large difference between the methoxy-modified donors and the plain TPA-based sensitizers. Interestingly, **D7** shows a reduced IPCE spectrum coverage, which is difficult to explain.

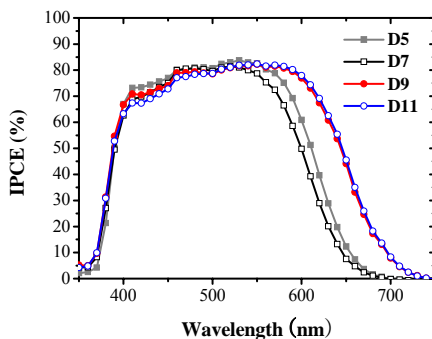


Figure 28. IPCE spectra of donor series.⁵⁵

The solar energy to electric current conversion efficiency of these sensitizers corresponds well to the IPCE, with **D9** and **D11** as highly efficient sensitizers (table 5).

⁵⁴ Absorption measurements performed by Tannia Marinado.

⁵⁵ IPCE, electrochemical and solar cell performances measurements performed by Jun-Ho Yum and Hyojoong Lee.

Table 5. Current and voltage characteristics of DSCs.⁵⁵

Dye	J_{sc} (mA/cm ²)	V_{oc} (mV)	ff	η (%)
D5	12.00	688	0.72	5.94
D7	11.00	695	0.71	5.43
D9	14.00	694	0.71	6.90
D11	13.50	744	0.70	7.03

In order to see the impact of the high molar extinction coefficient of these sensitizers on photovoltaic properties, TiO₂ films with various thicknesses, using **D11** sensitizer was investigated. The photocurrent increased with the thickness of the TiO₂ nanocrystalline layer. On the other hand, the photovoltage decreased with increasing thickness (table 6). The increase in surface area due to higher thickness of TiO₂ film allows for better light harvesting, but a higher possibility for injected electrons to recombine with the oxidized species such as triiodide. The devices using a 2.5 μ m thin TiO₂ layer yielded remarkably high photocurrent and IPCE of 12.3 mA/cm² and 79%, respectively, which we attribute to the high molar extinction coefficient of the dye.

Table 6. Current-voltage characteristics obtained with **D11** sensitized solar cells as various thicknesses of the nanocrystalline TiO₂ films.⁵⁵

Thickness (μ m)	J_{sc} (mA/cm ²)	V_{oc} (mV)	ff	η (%)
2.5 + 5	12.30	765	0.70	6.59
5 + 5	12.90	753	0.70	6.80
7 + 5	13.50	744	0.70	7.03
10 + 5	13.70	740	0.70	7.10

5.2.3. Solid State Solar Cell Performance of Donor Series

D5, **D7**, **D9** and **D11** were evaluated as sensitizers on the solid-state dye sensitized solar cells in which spiro-MeOTAD hole-conductor is used as a redox couple.¹⁹ Under standard global AM 1.5 solar conditions, all the **D**-series sensitized cells showed almost a half value of their liquid-electrolyte counterparts in overall efficiency while **D9** gave the best performance (see table 7). The IPCE of the **D9** sensitized device exhibited relatively high value of 40~50% in the range of 420 nm to 530 nm (figure 29), which is higher than the standard **N719**-based cell.¹⁹ Considering the film thickness (1.7 μ m) of TiO₂ used, the results from **D**-series sensitizers look promising in the application of solid-state cells.

Table 7. Current-voltage characteristics obtained with **D5**, **D7**, **D9** and **D11** sensitized solid state cells.⁵⁵

Dye	J_{sc} (mA/cm ²)	V_{oc} (mV)	ff	η (%)
D5	6.31	865	0.57	3.11
D7	5.02	785	0.71	2.79
D9	7.72	756	0.56	3.25
D11	5.85	811	0.63	3.01

It is interesting to note that the dyes containing methoxy donor groups (**D9** and **D11**) showed a better result than the corresponding dye without methoxy group (**D5** and **D7**). However, the sensitizers with only one TPA donor moiety (**D5** and **D9**) showed the highest efficiencies.

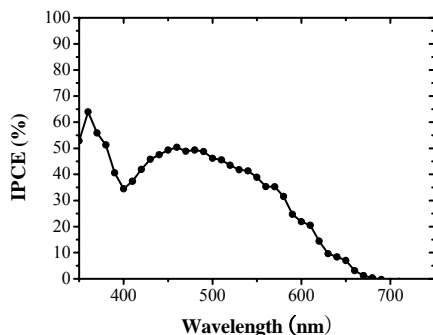


Figure 29. Solid state IPCE spectra of **D9** sensitizer.

By investigating the results of metal-free organic dye used solid state cells reported so far, the best dye in the donor series (**D9**) can be ranked in second place next to indoline dye **D102** (depicted in figure 5, chapter 1), which showed an efficiency of 4.1%.¹⁹ Although **D9** dye has a lower extinction coefficient ($\epsilon = 33000 \text{ dm}^3 \text{ mol}^{-1} \text{ cm}^{-1}$ at 462 nm) than that of **D102** ($\epsilon = 55800 \text{ dm}^3 \text{ mol}^{-1} \text{ cm}^{-1}$ at 491nm), the same photocurrent ($\sim 7.7 \text{ mA/cm}^2$) was obtained from **D9** and **D102**. This comparison indicates that **D9** has a better absorbed photon to current conversion efficiency than **D102** using the same type of solid-state cell.¹⁹

5.3. Conclutions

By introducing electron-donating groups on the donor part of the dyes, the solar cell performances are improved lowering the HOMO and LUMO energy level gap. The effect of the introduction of an extra donor moiety is less clear. In the case of an extra donor moiety without the electron donating methoxy groups (**D7**) the efficiency of the solar cell and the absorption decreases. However, by introducing an extra donor moiety with the electron donating methoxy groups (**D11**) the efficiency and the absorption increases. Further investigations with different electron donating groups in *para*-position of the TPA moiety are to be made.

6. Future Prospects

From the results reported, it is obvious that a number of optimizations can be made. On the donor side, various modifications on the TPA framework can easily be accomplished, for instance introducing dimethylamine in the *para*-positions or different heterocyclic and aromatic substituents. An alternative donor moiety, such as different indolines, carbazoles or phenothiazine should also be investigated.

The linkers can also be alternated with for instance phenyl, pyrrole and other hetrocyclic compounds. More interesting at this point is to prevent recombination of electrons from the semiconductor to the electrolyte. This can be achieved by introducing alkyl chains in the linker part of the dye, forming an insulating layer yielding an increased electron lifetime in the DSCs.²³ The alkyl chains are also believed to prevent aggregate formation on the surface of the TiO₂.

Insulation of the dyes in the solar cell could also be achieved by incorporating the chromophore into a macromolecular ring (figure 30). The **CD** macromolecule has been heavily investigated for the use as insulator of a wide variety of molecular wires, conducting polymers and organic semiconductors.⁵⁶ The insulation of chromophores in the cavity of different **CD** molecules has so far, to the best of our knowledge, not been investigated for use in the dye-sensitized solar cells, where the macromolecule is locked on the linker moiety by the donor and the acceptor group attached to the semiconductor.

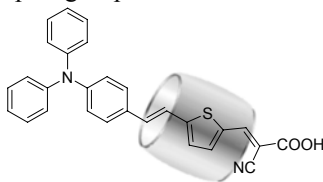


Figure 30. Schematic picture of **D5** sensitizer encapsulated in a **CD** macromolecule.

Some preliminary tests have been made, but so far have no effects been achieved in the photovoltaic performance of the solar cell.

⁵⁶ For a general review see: Frampton, M. J.; Anderson, H. L. *Angew. Chem. Int. Ed.* **2007**, *46*, 1028-1064.

7. Concluding Remarks

The number of possible combinations of donors, linkers and acceptors of chromophores for dye sensitized solar cells is huge. Presented here is a useful strategy to obtain highly efficient sensitizers by independently alternate the donor, linker or acceptor moiety. This will in the longer run help us to attain a “HOMO and LUMO energy level library”, where different group’s contribution can be collected.

So far, the best chromophore for liquid dye sensitized solar cells (**D11**) gives a solar energy to electric current efficiency (η) of 7.1%. In the solid state solar cell, efficiencies up to 3.25% have been reached which at this point places us in second place in the world.

Linker modifications and especially linker extension can give undesired side effects on the overall solar cell performances, such as electron leakage from the semiconductor to the electrolyte due to insufficiently surface coverage. However, the linker extension is a powerful tool to finetune the HOMO and LUMO energy levels of the sensitizers.

At this point only one additional acceptor moiety except the cyanoacrylic acid has been investigated, namely rhodanine-3-acetic acid. This shows a strong influence on the HOMO and LUMO energy levels due to the extension of the π -conjugated system. However, the electron coupling between the LUMO and the conduction band of the semiconductor is limited due to the saturated property of the anchor group, interrupting the π -conjugation. Further investigations should be made, and these sensitizers should be tested in the solid state solar cells.

Acknowledgements

I would like to express my sincere gratitude to:

Professor Licheng Sun, for accepting me as a PhD student, giving me guidance and letting me, sometimes, go my own ways.

Professor Anders Hagfeldt, always having time for inspiring and encouraging discussions.

Professor Björn Åkermark, for scientific ideas and discussions, even though I refuse going manganese!

Licheng, Ki, Gerrit, Staffan and Marcus for proof reading this thesis.

Tannia as colleague and friend. It's great working with you in the fight for higher efficiencies.

All past and present members of the Licheng group, especially Shiguo, Yunhua, and Dapeng for the nice atmosphere, Martin and Qin Peng for the long but pleasant hours in the lab and Samir for laughter's and keeping the entropy at a peak.

All past and present members of the Hagfeldt group, especially Gerrit and Tomas for nice collaborations. Tore Brinck, thank you for valuable discussions and for the calculations.

Dr. Nazeeruddin, professor Michael Grätzel and the Lausanne crew, for interesting collaborations and high efficiencies.

Haining, Ruikui and Xichuan in Dalian, for collaborations and taking care of a lost Swedish soul in China.

All past and present co-workers at the department of organic chemistry.

Marcus, for spreading a nice atmosphere.

Tessie, for all the gossip.

Staffan, PS2 gaming and chemistry advises.

All my friends on the outside, you are the waterhole in my spiritual desert.

The Karlsson family, for holidays, hunting and fun.

Mamma, syrran och grabbarna, you are always there when I need you.

Hanna, for every single day.

Appendix A

The following is a description of my contribution to Publications **I** to **IV**, as requested by KTH.

Paper I: I contributed to the formulation of the research problems, performed the synthesis and wrote parts of the manuscript.

Paper II: I contributed to the formulation of the research problems, performed a majority of the synthesis and wrote parts of the manuscript.

Paper III: I contributed to the formulation of the research problems, performed the synthesis and wrote parts of the manuscript.

Paper IV: I contributed to the formulation of the research problems, performed parts of the experimental work and wrote parts of the manuscript.